



Grant Agreement No. 611373



FP7-ICT-2013-10

### **D1.2.2. Enhanced communication transceiver units, protocols and software**

Due date of deliverable: 02/2015

Actual submission date: 03/2015

Start date of project: 01 January 2014

Duration: 36 months

Organization name of lead contractor for this deliverable: UNEW

Revision: version 1

Dissemination level		
PU	Public	x
PP	Restricted to other programme participants (including the Commission Services)	
RE	Restricted to a group specified by the consortium (including the Commission Services)	
CO	Confidential, only for members of the consortium (including the Commission Services)	

## Contents

1	Outline of the deliverable .....	2
2	Hardware enhancements .....	2
3	Enhancements to ultra- short baseline (USBL) positioning algorithm .....	5
4	Medium data rate spread spectrum communication .....	6
5	Communication protocols .....	11
6	Conclusions.....	11

## 1 Outline of the deliverable

This deliverable deals with the description of the enhanced communication transceiver units, with improved transducer construction, improved USBL positioning algorithms and optimized protocols. It also describes the finalized transmission scheme and receiver algorithms for a medium bit rate link (~1.4kbits/s) which are ready for deployment on the Seatrac devices. Results from various field experiments are presented to assess both communication and positioning performance are presented.

## 2 Hardware enhancements

The electronic design of the Seatrac units delivered in D1.2.1 has proven to be robust, powerful and flexible (via software changes). Hence no significant changes were considered necessary other than changing the pressure range of the integral depth sensor to provide maximum accuracy for the shallow water operations envisaged during CADDY.

The main area of hardware development has been in the construction of the USBL array transducer elements to maximise accuracy of phase measurements and repeatability in construction. Initial USBL units delivered to UNIZG had transducer elements selected from a production batch to be well matched in phase response. However, to enable consistent positioning performance on all units within the CADDY consortium and to support the ongoing SEAt rac commercialisation, it was necessary to review the design of these transducers to try to eliminate variability.



Figure 3.1 shows the results of USBL array calibration in UNEW's anechoic testing tank with a transponder 1m away and at the same depth. The plots show the phase differences between each pair of elements (baseline) in the 4 element array, (a) showing the baselines which are co-planar in the horizontal plane and (b) showing the baselines which have vertical separation. As the USBL head is rotated through 360 degrees, plots (a) and (b) should show 3 sinusoidal traces with 120 degree offsets, zero mean and no value exceeding +/-136 degrees. The device tested shows substantial deviation from the expected result due to differing transducer element response. Plot (c) shows the effect this has on the computed azimuth and elevation angles with large deviations

in the expected pattern (elevation should stay at zero and azimuth should ramp linearly between 0 and 360 degrees). Plot (d) shows the "fit error" which is a measure of the confidence in the computed fix.

After reviewing the transducer design it was decided to modify construction so that the ceramic elements were mounted on a small seat of acoustically matched polyurethane before over-moulding with the same material. This would eliminate any interaction with the mounting structure which was suspected to be the cause of variable response. Figure 3.2 shows the calibration result of a USBL head with the new transducer construction. We can see that the baseline phase shifts are now much closer to the theoretically predicted result as are the calculated azimuth and elevation angles (the remaining fluctuation in elevation angle can be largely attributed to the imprecise mechanical arrangement for rotation of USBL heads in the tank). The fit error is also seen to be substantially lower across all angles.



The improved transducer construction will be used in all future Seatrac units for the CADDY project and existing units will be upgraded as soon replacement units are available.

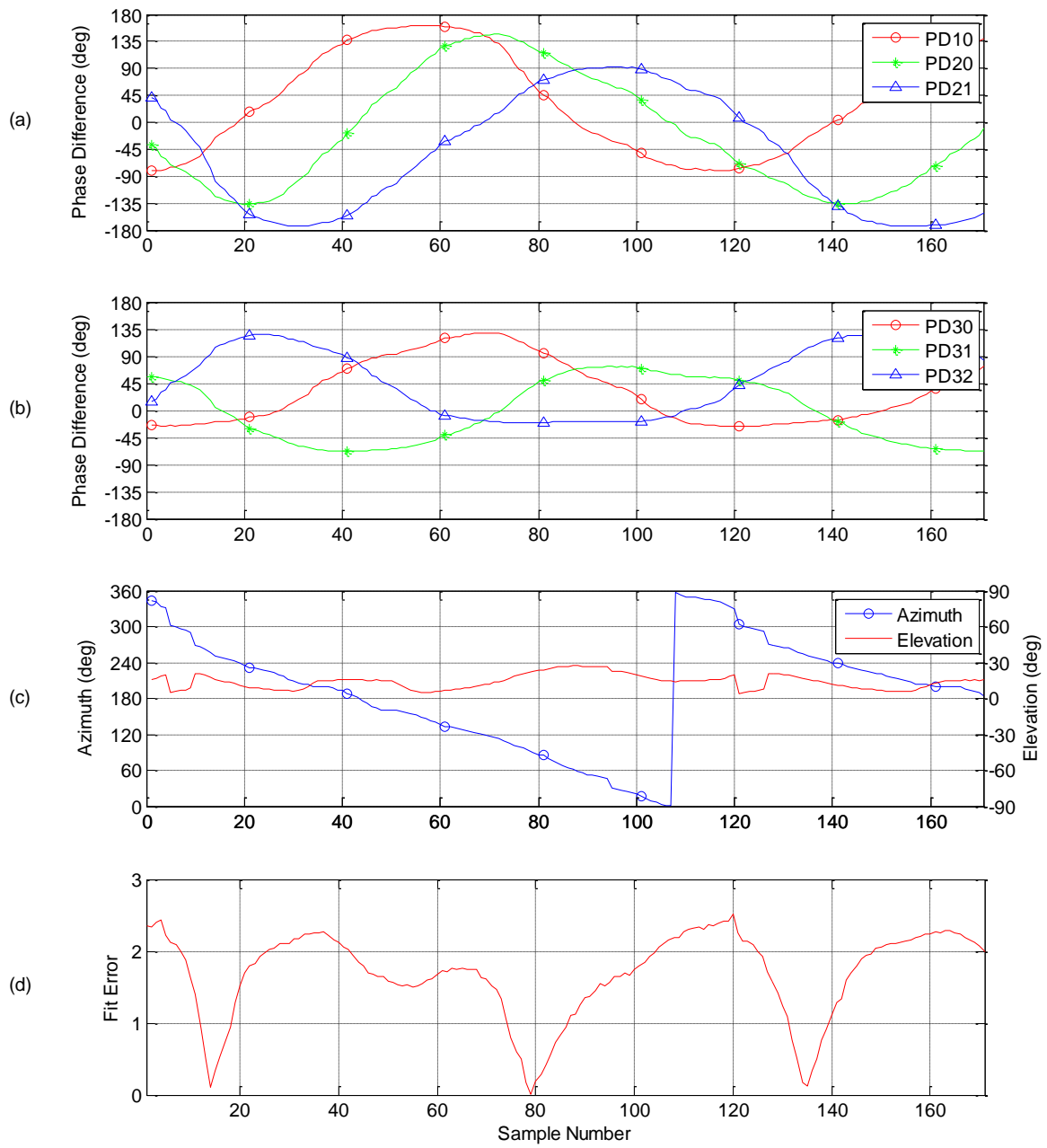


Figure 3.1 – USBL array calibration results with old transducer construction

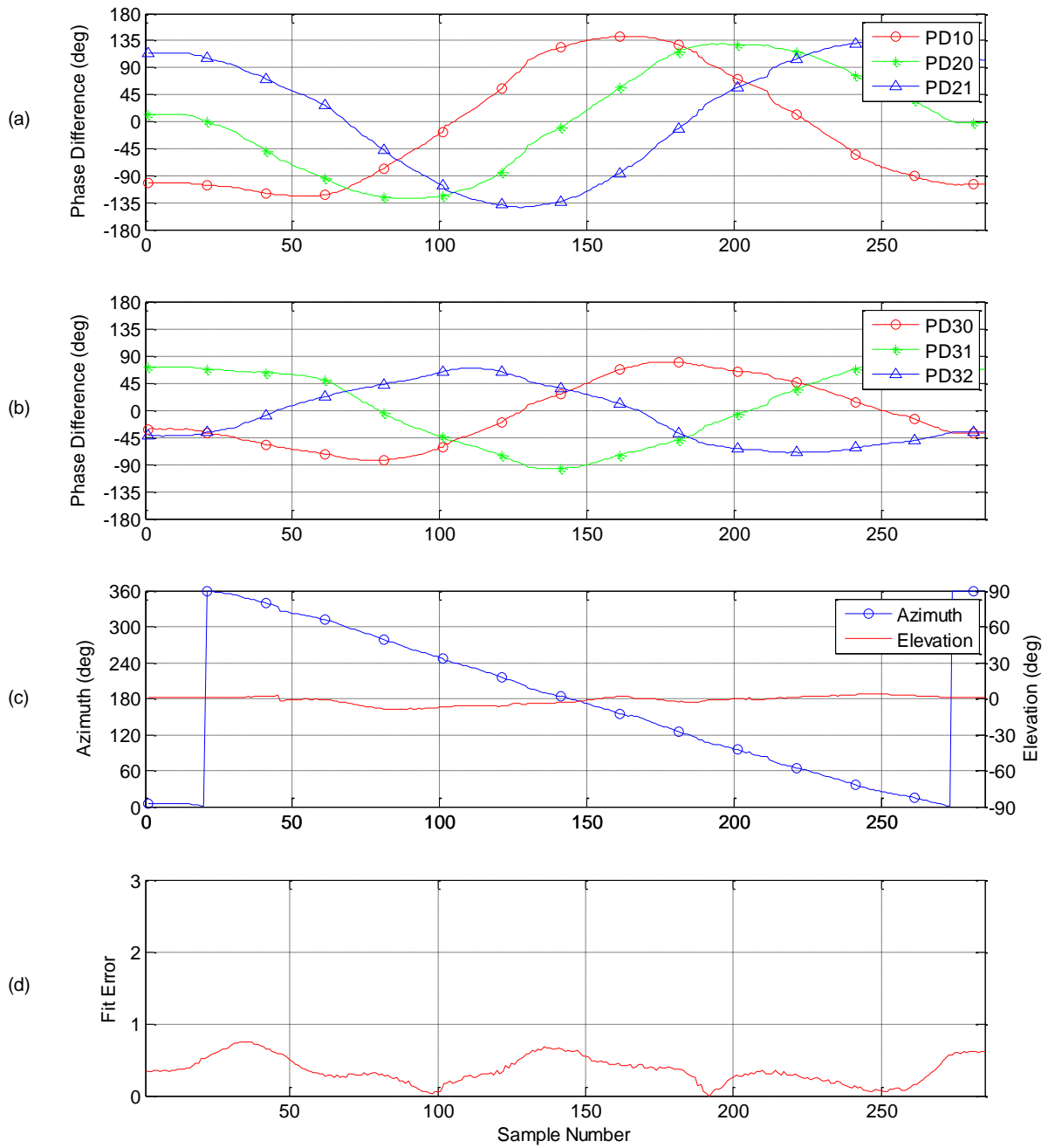


Figure 3.2 – USBL array calibration results with new transducer construction

### 3 Enhancements to ultra- short baseline (USBL) positioning algorithm

Although positioning results for the initial Seatrac devices were very encouraging, various experiments described in D1.2.1 indicated ways that the algorithms could be further improved to increase accuracy and repeatability of fixes. One potential issue was how the algorithm synchronises onto closely spaced multipath arrivals as shown in figure 4.1. It is intuitive to synchronise on the signal with the greatest energy (and hence SNR) but the complexities of underwater propagation often result in a multipath signal that is stronger than the most direct path. Locking onto a multipath signal can often result in inaccurate position fixes as the direction of arrival does not match the direction of the source. This is particularly problematic when multiple paths fluctuate in amplitude and swap rank, resulting in fluctuating fixes.

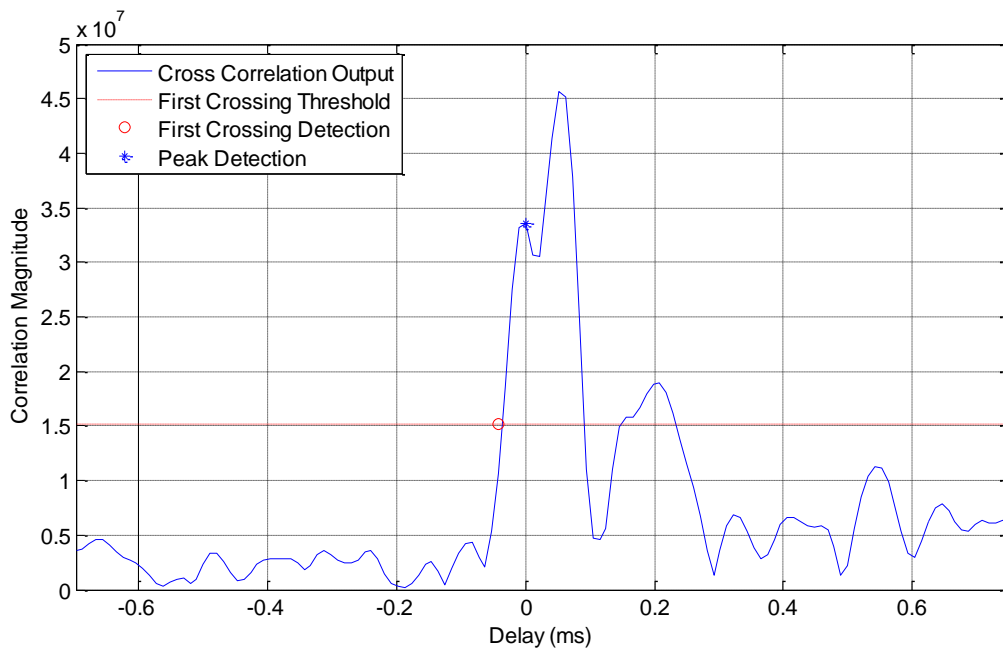


Figure 4.1- channel impulse response showing USBL synchronisation

The USBL algorithm has now been modified to guarantee that the USBL uses the first acoustic arrival (most accurate) to calculate position fixes. The algorithm now calculates a dynamic threshold based on the largest arrival amplitude and uses this to detect the rising edge of the first signal path, regardless of the multipath profile. A peak finding algorithm is then used to locate the maxima of this first arrival which is the optimum value for USBL calculation.

The improved USBL algorithm and transducers were tested in a dock near Newcastle with floating pontoons in a regular grid pattern. Figure 4.2 shows the position fixes obtained (50 in each location) relative to the USBL at coordinate (0, 0) with the X-Y, plane and the Y-Z planes displayed. Ground truth positions from the map are indicated by a red asterisk. The standard deviation ( $\sigma$ ) of fixes (in 3 dimensions) is also plotted against range for each position, indicating a value of about 1.5% of range. As expected for a USBL system, this is dominated by the variance of azimuth and elevation angle rather than the ranging accuracy. In order to decouple the acoustic fix accuracy from attitude sensor (AHRS) accuracy, the AHRS is disabled and a fixed attitude is estimated. The apparent geometric distortions seen around the 10-40m are most likely due to errors in the assumed attitude due to inaccurate orientation of the testing rigs used. Further optimisation of the USBL algorithms will continue based on this data set and others.

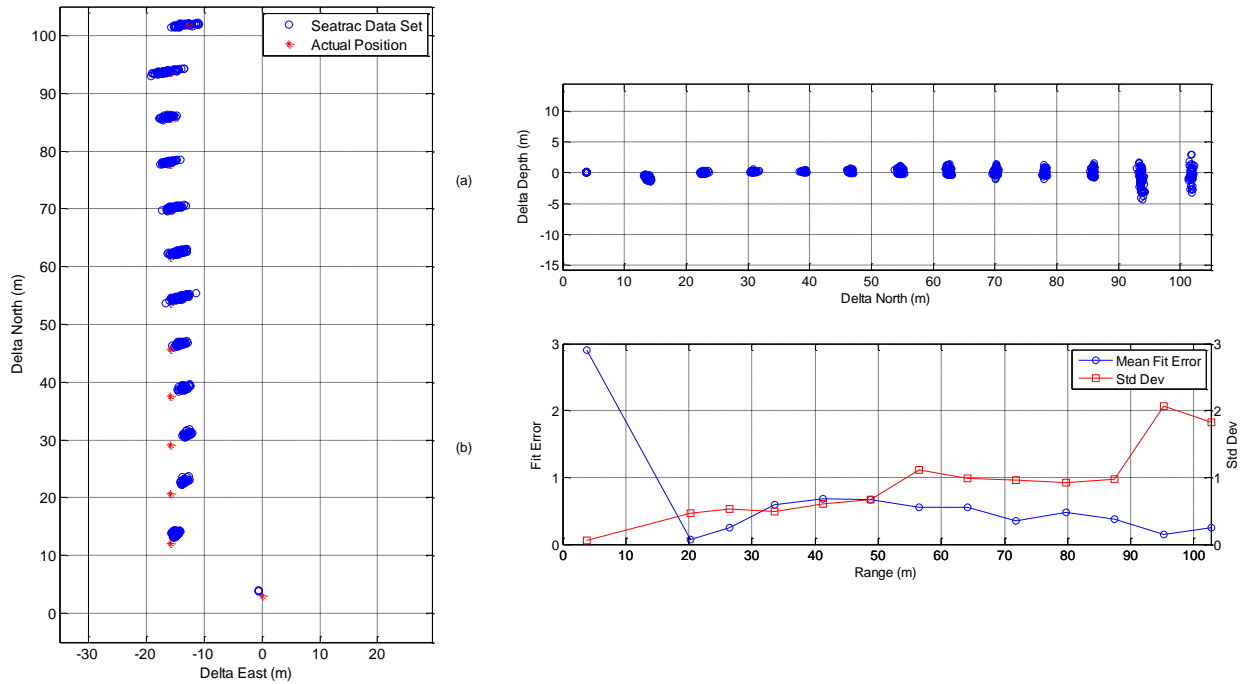


Figure 4.2 – Results of dock testing of Seatrac USBL with regular pontoon layout

#### 4 Medium data rate spread spectrum communication

In D1.2.1 the modulation and receiver structure for a medium bit rate acoustic communication link, based on the principles of direct sequence spread spectrum (DSSS), was described. Here a detailed description of the finalised modulation, encoding, packet formats and receiver algorithms is presented along with test results to assess the robustness of the transmission scheme in the presence of severe multipath, Doppler effects due to platform motion and noise. The emphasis of this design is to achieve high reliability using only a single receiver hydrophone whilst keeping the computational complexity of the receiver within the capability of the miniature, low cost Seatrac platform.

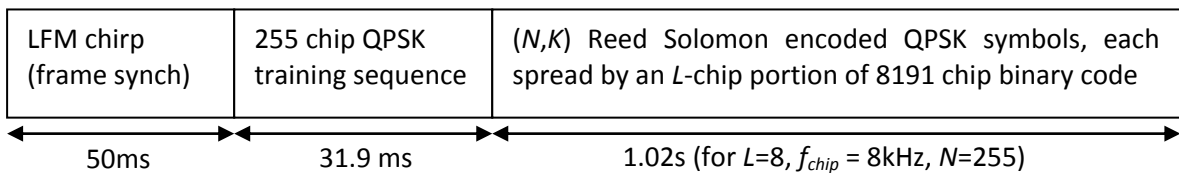


Figure 5.1 – Transmitted packet format for DSSS acoustic link

The structure of a transmitted data packet is shown in figure 5.1. Each packet starts with a 50ms long linear frequency modulated (LFM) chirp waveform for frame synchronisation. This is followed by a 255 chip QPSK modulated sequence, derived from a maximal length binary code (M-sequence), which is used to train the adaptive filter and Doppler correction structure in the receiver. Finally Reed Solomon (RS) encoded data is modulated as a series of QPSK symbols, each spread by an  $L$ -chip segment of a longer 8191 point binary M-sequence. As later results will show, although this spreading gain cannot on its own guarantee to remove inter-symbol interference (ISI), it is consistently able to reduce the mean ISI to a level where the error correction coding can eliminate

remaining errors. By varying the values of  $L$  and the RS code rate ( $K$ ), spread spectrum processing gain and coding gain can be easily tuned to balance data throughput against channel conditions. The transmitter and receiver structures are described in figures 5.2 and 5.3 respectively.

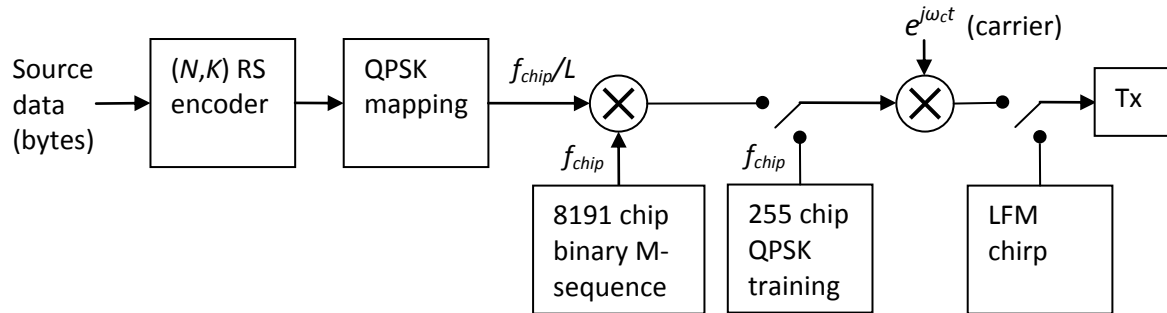


Figure 5.2 – DSSS transmitter structure

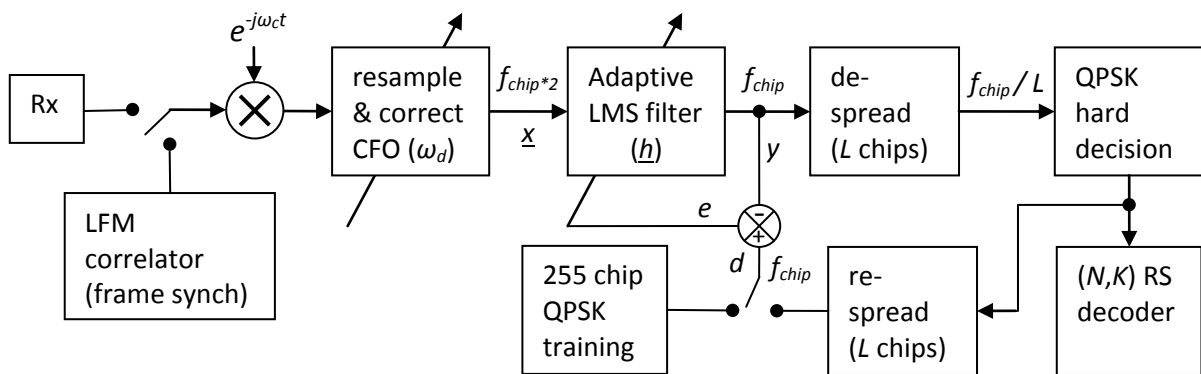


Figure 5.3 – DSSS receiver structure

The receiver first synchronises to the start of a transmitted packet by correlation for LFM frame synch waveform. The signal is then down-converted to a complex baseband signal and resampled by a factor  $R$ , using linear interpolation, to remove Doppler effects. This Doppler correction step also includes the removal of carrier frequency offset (CFO) estimated as  $\omega_d$ . The estimation of both the resampling factor and carrier frequency offset is discussed later. The re-sampler outputs 2 samples per chip which are fed into a linear adaptive filter.

The output of the adaptive filter is calculated at one sample per chip according to equation (5.1). The purpose of this filter is twofold: primarily to maintain precise phase and chip synchronisation but also to provide equalisation, combining the energy from multipath arrivals to increase the achievable signal to interference and noise ratio (SINR). Whilst complex non-linear equaliser structures can be effective on quite long delay spreads up to perhaps 100 symbols, the intention here is that the DSSS processing gain will be able to attenuate multipath of almost limitless delay spread. Hence the adaptive filter is restricted to <40 taps to minimise computational load and maximise stability at low SNR. Nevertheless this does provide a useful gain through equalisation of short delay multipath arrivals. After the adaptive filter, the synchronised and equalised chip sequence is then de-spread to recover the estimated QPSK symbols, a hard decision is made and the data finally decoded.

The adaptive filter coefficients are updated at the chip rate to maximise tracking ability. The error signal is calculated as in equation (5.2), where  $d[i]$  is the transmitted chip value which is either taken from the a priori known training sequence or is estimated by re-spreading the QPSK hard decision output with the a priori known spreading sequence (decision directed mode). The adaptive filter coefficients are then updated as in equation 5.3, using the computationally simple least mean squares (LMS) algorithm, where  $\mu$  is the adaptive step size.

$$y[i] = \underline{h}^T [i] \underline{x}[i] \quad (5.1)$$

$$e[i] = d[i] - y[i] \quad (5.2)$$

$$\underline{h}[i + 1] = \underline{h}[i] + \mu e[i] \underline{x}^* [i] \quad (5.3)$$

The resampling factor, R, for Doppler correction must also be adapted. The phase error on the output symbols is calculated, as in equation (5.4), and this becomes our cost function for minimisation. A straightforward proportional feedback loop is then used to update the resampling factor as in (5.5), where  $k_p$  is the proportional tracking constant. Finally the CFO ( $\omega_d$ ) is proportional to the estimated resampling factor and calculated as in equation (5.6).

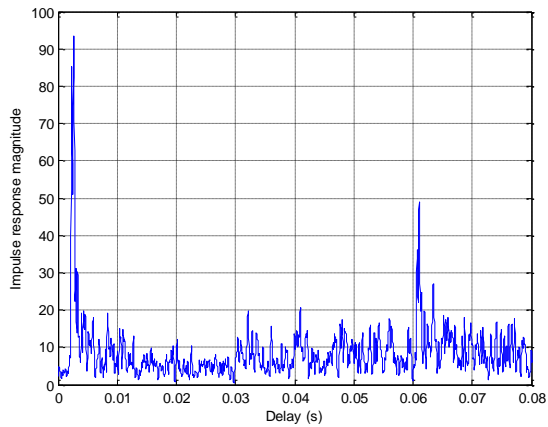
$$\theta_e[i] = \arg(y[i] \cdot d^*[i]) \quad (5.4)$$

$$R[i + 1] = R[i] + k_p \theta_e[i] \quad (5.5)$$

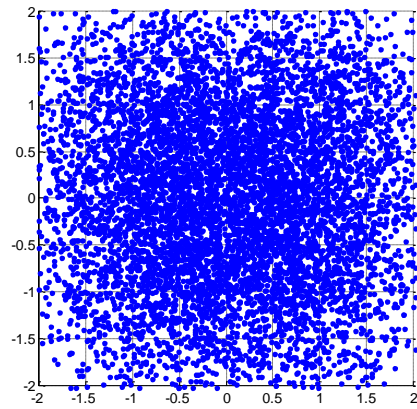
$$\omega_d = \omega_c (R[i] - 1) \quad (5.6)$$

<b>Parameter</b>	<b>Symbol</b>	<b>Value</b>
Carrier frequency	$f_c$	12kHz
Acoustic frequency band	-	8-16kHz
Chip rate	$f_{chip}$	8000
Spreading ratio (chips/symbol)	$L$	8
RS code rate	$(N,K)$	(255,191)
Training sequence length	-	255 chips
Net data throughput	-	1.39 kbits/s
LFM chirp	-	8-16kHz, 50ms duration
Adaptive filter length	-	36 taps
Adaptive step size	$\mu$	0.02 training, 0.005 for data
Doppler tracking constant	$k_p$	$2 \times 10^{-5}$ training, $5 \times 10^{-6}$ for data

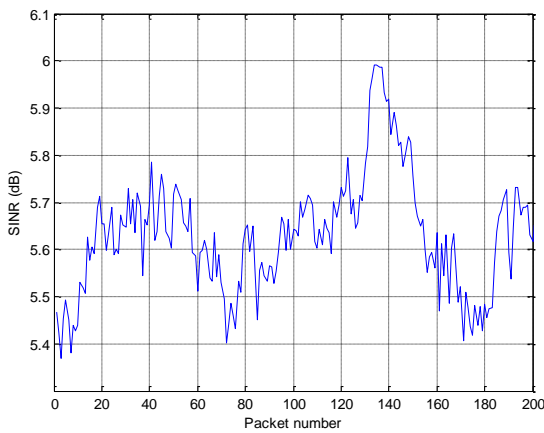
Table 5.4 – Parameters for DSSS experiments



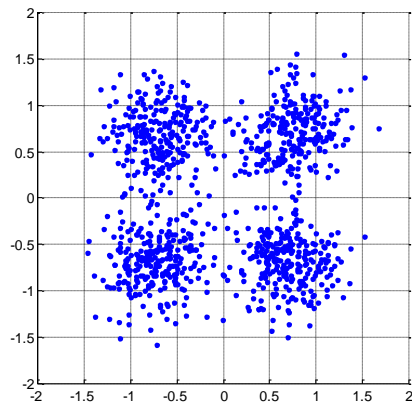
(a) Example channel impulse response



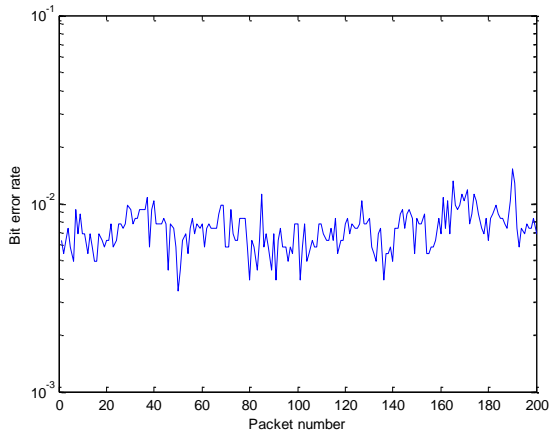
(d) Chip I-Q constellation



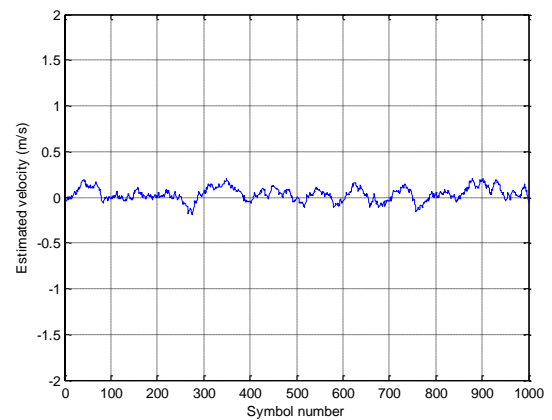
(b) SINR over 200 received packets



(e) Symbol I-Q constellation



(c) Bit error rate before decoding



(f) Estimated velocity from Doppler tracking

Figure 5.5 – results of 100m DSSS transmission experiment in highly reverberant dock environment

Initial test results of the basic DSSS scheme was presented in the D1.2.1 document and these were used to establish the best set of parameters for a system implementation. Further experiments were conducted during October 2014 to fully explore the performance of this scheme in extremely challenging multipath conditions, posed by an enclosed concrete lined dock, and with erratic source velocity and acceleration induced to simulate deployment on a diver or agile underwater vehicle. The parameters used in these experiments are listed in table 5.4.

Figure 5.5 shows the results of a static test over 100m range, illustrating the high resilience to multipath effects of the DSSS scheme. Figure 5.5(a) shows the channel impulse response with significant signal arrivals spanning at least 80ms. Such a channel is extremely difficult to deal with by equalisation alone and would require many hundreds of filter taps. Figure 5.5(b) shows an example constellation plot for the estimated chips in one packet, indicating a completely closed eye. However the constellation of the symbol values, after de-spreading, shows a much improved result leading to acceptable SINR (figure 5.5(b)) and a sustained mean bit error rate of less than  $10^{-2}$ . After RS decoding, all 200 of these packets are received error free achieving a sustained throughput of 1.39kbts/s.

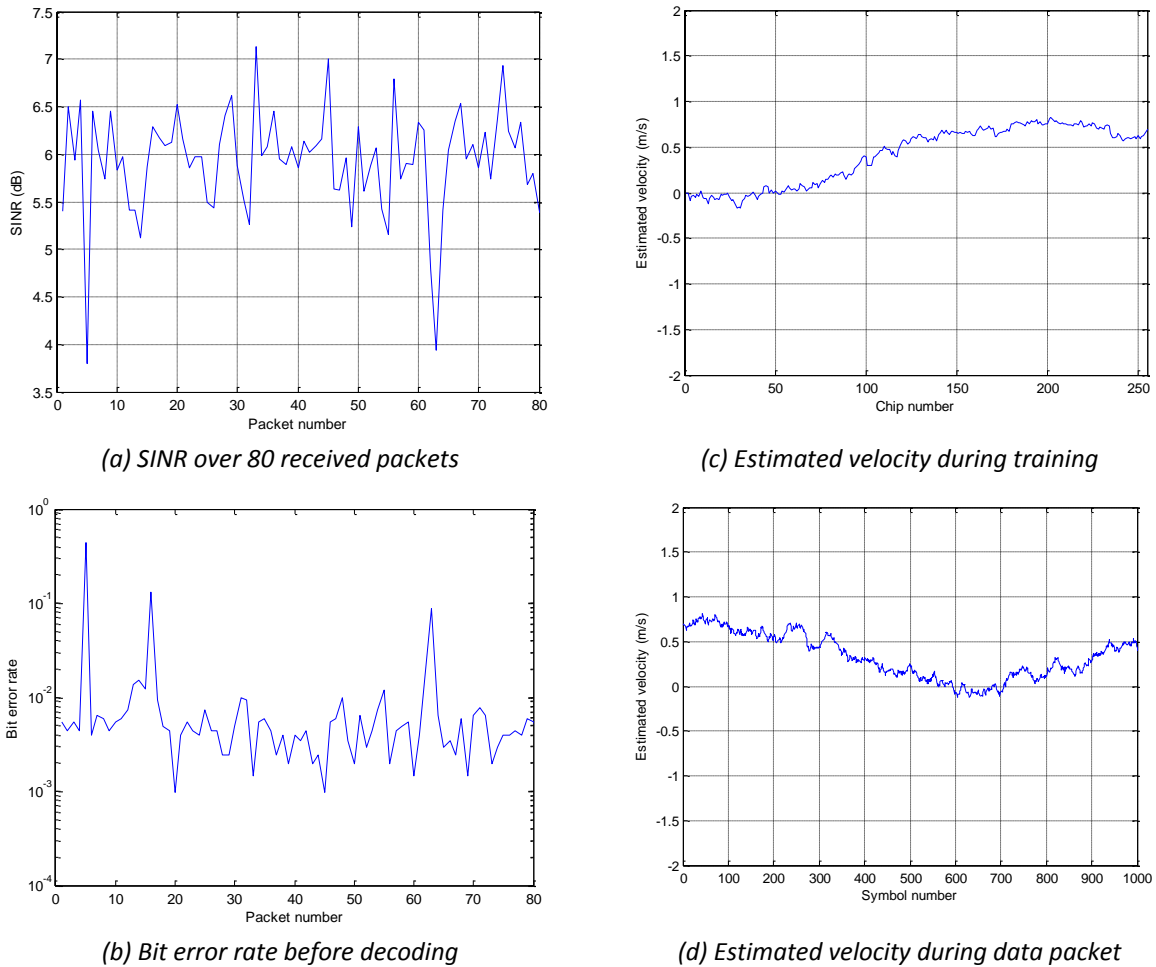


Figure 5.6 – results of DSSS transmission experiment with time varying Doppler effects

Figure 5.6 shows the results of a transmission experiment, in the same reverberant dock environment, while random motion was induced in the transmitting unit resulting in accelerations frequently exceeding  $2 \text{ m/s}^2$ . Figure 5.6 (a) and (c) show the SINR and bit error respectively over 80 transmitted packets, with 77/80 packets decoded error free. Figure 5.6 (c) shows the acquisition phase of the Doppler tracking algorithm during the training sequence and figure 5.6(d) shows how the algorithm continues to track varying velocity during the reception of a data packet. This synchronisation method proves to be critical for the success of the DSSS system with only 22/80 of the same packets successfully decoded without it.

The medium rate DSSS transceiver design has proven extremely robust in a wide range of realistic test scenarios, whilst satisfying the low computational load requirements for implementation on the

SEAtac platform. The algorithm is now being ported onto the SEAtac hardware to provide upgraded data rates for the next set of CADDY vehicle/diver trials.

## 5 Communication protocols

The boost in performance and reliability provided by the underlying hardware, has allowed the upper layer of the acoustic communication protocol (as previously defined in D1.2.1) to improve its performance as well. The main focus of these improvements concerns the optimization of the information coding and the prioritization of messages to be sent on the acoustic channel.

Referring to D1.2.1 requirements, *soft real-time performance* has improved mainly because the enhanced data rate of transceivers leads to shorter transmission delays and shorter (and less likely) timeout events in case of packet loss. *Prioritization and QoS* (Quality of Service) of safety-critical information is still necessary but its enforcement causes fewer events of essential information loss. To further minimize these events, safety-critical bits of information are now acknowledged by the recipient of the message. This is now the only *error detection* mechanism left in the upper layer of the protocol, while no *error recovery* mechanisms are enforced in the final version of the communication protocol.

The *entropy* and *compression* of the data about to be sent has been improved mainly for what concerns user-generated data (e.g. text strings to be sent to/from the diver and the surface control station) that is now compressed using static Huffman tables optimized for the English language. This approach avoids the complex training and exchange of dynamic Huffman codebooks, that are in fact quite hard to be made general enough to be successfully adapted to highly heterogeneous datasets and operation conditions.

It's important to note that, when talking about the underwater medium, savings in terms of packet size are strongly related to a decrease in packet loss probability, so even a few bytes of compression gain can be considered a good result. For these reasons, the same optimization strategies will be considered for what concerns the output of the finalized symbolic language interpreter. If preliminary tests will show a substantial gain in bandwidth savings, language symbols and data will be encoded, compressed and/or subject to quantization before being sent through the acoustic link.

## 6 Conclusions

This deliverable has reported the description of the enhanced communication transceiver units, with improved transducer construction, improved USBL positioning algorithms and optimized protocols. It has also reported the finalized transmission scheme and receiver algorithms for a medium bit rate link (~1.4kbits/s) which are ready for deployment on the Seatrak devices.

A number of field experiments have been reported in order to assess both communication and positioning performance.

Upgrades related to communication protocol features are evaluated on the basis of hardware and low level services updates.